Wetting behavior above the liquid-crystal–isotropic transition in a homologous series

R. Lucht and Ch. Bahr*
Institute of Physical Chemistry, University Marburg, D-35032 Marburg, Germany

G. Heppke
I.-N.-Stranski-Institute for Physical and Theoretical Chemistry, Technical University Berlin, D-10623 Berlin, Germany

(Received 17 February 2000)

An ellipsometric study of the wetting behavior at the free surface above the isotropic to nematic or isotropic to smectic-*A* transition of nine homologous compounds with even alkyl chain lengths *n* in the range from four to twenty carbon atoms is presented. All compounds show a pretransitional increase of the nematic or smectic surface coverage as the bulk isotropic to liquid-crystal transition is approached from above. The behavior of the nematic compounds ($n=4$ to 10) can be interpreted, within the framework of a Landau model, as complete wetting. In short nematic homologs the divergence of the nematic coverage is strongly reduced by a decrease of the nematic susceptibility of the isotropic phase. The elastic coefficient *L* of the Landau model shows a pronounced increase with increasing *n*, resulting in the occurrence of a discontinuous prewetting transition in the shortest smectic homolog ($n=12$) that is still describable by the nematic Landau model. In the longer smectic homologs ($n=14$ to 20), layering steps appear in the pretransitional increase of the coverage. The results indicate probable partial wetting for the longest homolog, whereas for the other smectic compounds the distinction between complete and partial wetting is difficult on the basis of ellipsometry.

PACS number(s): 64.70.Md, 68.10.−m, 68.45.Gd

I. INTRODUCTION

Thermotropic liquid crystals exhibit a wealth of surface phenomena [1,2] at both liquid-crystal–wall and liquid-crystal–vapor interfaces. The behavior at wall interfaces is of direct interest in the technological application of these materials and many studies are concerned with the corresponding orientational anchoring and wetting behavior of liquid crystals on solid substrates (see [3–12] and references in these works).

We focus here on the wetting behavior occurring at the free surface above the bulk liquid-crystal—isotropic transition. The first liquid-crystal phase below the isotropic liquid is in the vast majority of cases either a nematic or a smectic-*A* phase. In the nematic phase, the rodlike molecules tend to align along a common direction without showing any long-range positional order. In the smectic-*A* phase there is an additional density wave (or weakly defined layer structure) possessing a period of about one molecular length; the wave vector (or layer normal) is parallel to the mean direction of the long molecular axes.

The first indication of a liquid-crystalline free surface excess order in the bulk isotropic temperature range came from surface tension measurements [13] of the compound 5CB [14] which shows an isotropic-nematic transition. An ellipsometric study [15] of 5CB confirmed the presence of a nematic surface layer at the free surface of the isotropic phase; the thickness of the nematic surface layer was found to diverge logarithmically at the bulk isotropic to nematic transition, indicating complete wetting of the isotropic liquid-vapor interface by the nematic phase. Subsequent ellipsometry studies [16–18] of nematic *n*CB [14] and PCH*n* [19] compounds also yielded complete wetting behavior (with the possible exception of 5CB; see the discussion below in Sec. III A). The wetting behavior at the free surface above smectic-*A*–isotropic transitions has been studied for various smectic *n*CB and *n*OCB [20] compounds, mainly by x-ray reflectivity [21–23] but also by ellipsometry [18]. The x-ray measurements provided direct evidence of the presence of smectic layers at the surface; at the bulk isotropic–smectic-*A* transition temperature, a finite number of layers (five for 12CB, two for 16OCB) was detected, indicating a partial wetting behavior.

All liquid-crystal compounds mentioned above belong to the three homologous series of *n*CB, *n*OCB, and PCH*n* compounds, which possess a very similar molecular structure and a strong dipole moment resulting from a terminal cyano group. We have recently begun a study of a larger variety of nonpolar compounds and found a number of previously unobserved behaviors such as partial wetting (or nonwetting) without pretransitional increase of surface order or the occurrence of prewetting transitions [24–27]. Most of the compounds of these studies belong to the homologous series of the $\bar{n}.\mathrm{O}.\bar{6}$ compounds [28] and we present here a detailed study of this series comprising all even-numbered members in the range from $n=4$ to $n=20$.

II. EXPERIMENT

The molecular structure of the $\bar{n}.\mathrm{O}.\bar{6}$ compounds, which were prepared at the Technical University in Berlin, is shown in Fig. 1. Table I gives the phase sequences and transition temperatures. Only substances with an even number of

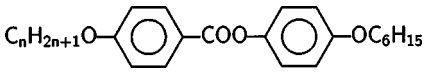

FIG. 1. Molecular structure of the $\bar{n}.\mathrm{O}.\bar{6}$ compounds.

*Corresponding author. Email address: bahr@mailer.uni-marburg.de

TABLE I. Transition temperatures (in °C) of the compounds under investigation. ● indicates the presence of a particular phase.

Compound	Smectic-*A*		Nematic		Isotropic
$\overline{4}$.O.$\overline{6}$			●	90.1	●
$\overline{6}$.O.$\overline{6}$			●	88.4	●
$\overline{8}$.O.$\overline{6}$			●	89.1	●
$\overline{10}$.O.$\overline{6}$	●	83	●	88.5	●
$\overline{12}$.O.$\overline{6}$	●	89.1			●
$\overline{14}$.O.$\overline{6}$	●	89.4			●
$\overline{16}$.O.$\overline{6}$	●	89.1			●
$\overline{18}$.O.$\overline{6}$	●	86.9			●
$\overline{20}$.O.$\overline{6}$	●	86.9			●

carbon atoms in the alkyl chain are studied; investigation of the odd-numbered homologs would certainly reveal some kind of odd-even effect (as observed in [18]) but probably no additional fundamental information.

A sketch of our experimental geometry is shown in Fig. 2. An approximately 1 mm thick film on a rough glass substrate is prepared. As substrate we use a microscope slide possessing on one side a rough surface (which is normally used for labeling the slide). A 1 mm thick stainless steel ring with an inner diameter of 1.5 cm is fixed with two-component epoxy glue on the slide. The freshly glued ''basin'' is heated to 150 °C for 24 h (to properly finish the chemical reaction in the glue) and then washed thoroughly with high-purity water, ethanol, acetone, and methylene chloride in order to remove any contamination.

The sample holder is filled with ≈200 mg of the liquid crystal and placed into an electrically heated two-stage brass oven which is additionally shielded by an aluminum case (which is not temperature controlled). Optical access is provided by small open slits; glass windows are avoided because the angle of incidence θ_i is varied (the polarization

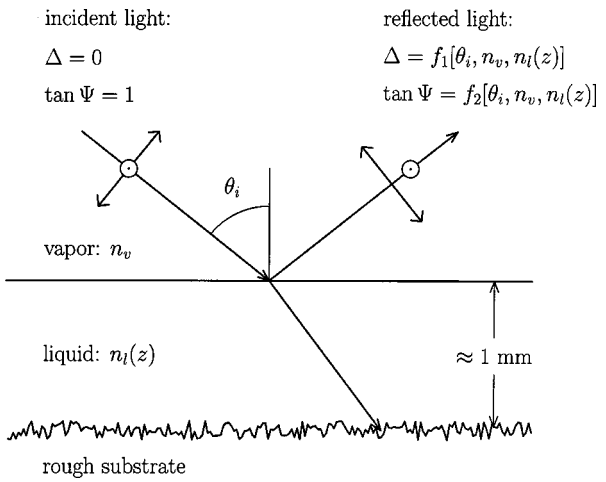

FIG. 2. Sketch of the experimental geometry. The polarization of the incident laser beam (θ_i: angle of incidence) is described by two linearly polarized components that possess equal amplitudes ($\tan\Psi = 1$) and are in phase ($\Delta = 0$). The polarization of the reflected beam depends on θ_i and the refractive index profile of the vapor-liquid interface. The rough substrate scatters the refracted beam in order to avoid interference with the first reflected beam.

effects of the windows are negligible only if the light passes perpendicularly through the windows). The temperature in the inner oven (which is controlled by a Lake-Shore 340 temperature controller) is measured by a YSI 44011 thermistor which is placed near the liquid-crystal sample. The temperature stability, as measured by the thermistor, is of the order of 5 to 10 mK.

Using a phase modulated ellipsometer we determine the ellipsometric angles Δ and Ψ that correspond to the argument and the absolute value of the complex reflection amplitude ratio r_p/r_s of the *p*- and *s*-polarized components of the reflected light:

$$\frac{r_p}{r_s} = \frac{|r_p|}{|r_s|} e^{i(\delta_p - \delta_s)} = \tan\Psi e^{i\Delta}, \tag{1}$$

with $|r_{p,s}|$ and $\delta_{p,s}$ corresponding to the (real) amplitudes and phases of the *p*- and *s*-polarized components. The polarization of the incident light can be described by $\Delta = 0$ and $\Psi = 45°$ [in fact, the polarization of the incident (and reflected) light is modulated during the measurement with a frequency of 50 kHz, but the Δ and Ψ values determined as described in the following give the polarization of the reflected light if the incident light was polarized as given above].

The principles of operation of a phase modulated ellipsometer are described in detail in [29]. The beam of a HeNe laser passes through a linear polarizer, which is fixed at an azimuthal angle of 45° with respect to the plane of incidence, and then through a photoelastic modulator (Hinds Instruments PEM 90) which modulates the phase difference δ_m between the *p*- and *s*-polarized components of the incident light as

$$\delta_m = \delta_0 \sin(2\pi\nu t) \tag{2}$$

with $\delta_0 = 138°$ and $\nu = 50$ kHz. The incident beam is reflected by the free surface of the sample and then passes a second linear polarizer, oriented at $-45°$. The light intensity behind the second polarizer is detected by an R928 photomultiplier. The signal voltage of the multiplier is fed into two lock-in amplifiers (Stanford Research SR830), which measure the amplitudes U_ν and $U_{2\nu}$ of the ac components with frequencies ν and 2ν of the multiplier output. Additionally, the dc component U_{dc} of the multiplier output is determined by a dc voltmeter.

All ellipsometer components are mounted on two optical benches (for the incident and the reflected beam) which can be rotated around a common axis. The rotation of the benches is achieved via stepping-motor-controlled linear positioners; the angle θ_i between the incident beam and the surface normal can be adjusted between 10° and 90° (with the presently used oven, this range is restricted to 45°–65°) with a resolution of the order of 0.001°. The angle of the second bench (for the reflected beam) is always adjusted to the specular position.

The light intensity *I* at the photomultiplier is a function of the modulator-induced phase difference δ_m and of the ellipsometric angles Δ and Ψ of the sample that we want to determine. The relation between the measured voltages U_ν, $U_{2\nu}$, U_{dc}, and Δ and Ψ is obtained via a series expansion

of the time-dependent part of I involving Bessel functions $B_n(\delta_0)$ of the modulation amplitude δ_0 (the reason for choosing $\delta_0 = 138°$ is that B_0 vanishes for this argument). One gets finally

$$\frac{U_\nu}{U_{dc}} = R_\nu^{cal} \sin\Delta \sin(2\Psi), \tag{3}$$

$$\frac{U_{2\nu}}{U_{dc}} = R_{2\nu}^{cal} \cos\Delta \sin(2\Psi). \tag{4}$$

The calibration factor R_ν^{cal} is determined by setting $\theta_i = 90°$ and replacing the sample by a $\lambda/4$ plate; the ellipsometric angles are then $\Delta = 90°$ and $\Psi = 45°$ so that a measurement of U_ν/U_{dc} directly yields R_ν^{cal}. The factor $R_{2\nu}^{cal}$ is determined in the same geometry but without the $\lambda/4$ plate and without sample; Δ and Ψ correspond then to the values of the incident light, i.e., $\Delta = 0$ and $\Psi = 45°$, resulting in $U_{2\nu}/U_{dc} = R_{2\nu}^{cal}$.

The values of Δ and Ψ of the reflected light depend on the refractive index profile along the surface normal of the sample. The best sensitivity is achieved when θ_i corresponds to the Brewster angle θ_B. In the case of an idealized sharp interface between two homogeneous dielectrics, the phase difference Δ jumps by 180° and the amplitude ratio $\tan\Psi = |r_p|/|r_s|$ is equal to zero because p-polarized light is not reflected at $\theta_i = \theta_B$. For a real interface, Δ is continuous and $\tan\Psi$ shows a value above zero at the Brewster angle, which is defined by Δ being equal to 90°. The value of $\tan\Psi$ at $\theta_i = \theta_B$ is usually designated as the ellipticity coefficient $\bar{\rho}$. In the present study, we always measure $\bar{\rho} > 0$ for two reasons. First, the finite width or roughness of a liquid surface produces a nonzero contribution $\bar{\rho}_0$ to $\bar{\rho}$. Describing the index profile $n(z)$ of the vapor (index n_v)–liquid (index n_l) interface by a Fermi profile of width γ,

$$n^2(z) = \frac{n_l^2 + n_v^2}{2} + \frac{n_l^2 - n_v^2}{2} \tanh\left(\frac{z}{\gamma}\right), \tag{5}$$

one finds $\bar{\rho}_0 \propto \gamma$ for γ in the range of a few nanometers [25]. Second, the presence of a surface layer with optical properties different from those of the bulk results in a contribution $\bar{\rho}_\Gamma$ to $\bar{\rho}$. The magnitude of $\bar{\rho}_\Gamma$ depends on the coverage Γ of the surface, which can be defined as

$$\Gamma = \int S(z)dz = \int [n_e^2(z) - n_o^2(z)]dz, \tag{6}$$

with $S(z)$ being the nematic order parameter profile and n_e and n_o the extraordinary and ordinary indices of refraction. One finds $\bar{\rho}_\Gamma \propto \Gamma$ for small values of Γ, corresponding to a surface layer thickness up to ≈ 50 nm for typical n_e and n_o values of liquid crystals; with further increase in Γ or surface layer thickness, $\bar{\rho}_\Gamma$ goes through a maximum and decreases again [25]. Thus, a divergence of Γ does not result in a divergence of $\bar{\rho}$ and complete and partial wetting are often difficult to distinguish by ellipsometry.

We should note that only in the case of a nematic wetting layer is Γ as defined above in a strict sense a quantitative measure of the coverage, since it does not take into account the positional ordering of the molecules in the smectic-A phase. For a smectic wetting layer, Γ measures only the total amount of orientational order at the surface. In the case of an isotropic to smectic-A transition, this is only a small drawback since the orientational order is an essential part of the liquid-crystal excess surface order; the above definition of Γ is not suitable for the case of smectic wetting above a nematic to smectic-A transition. However, Γ according to Eq. (6) corresponds exactly to the part of the excess surface order that is measurable by ellipsometry.

In order to determine $\bar{\rho}$ as a function of temperature T, values of Δ and Ψ are continuously measured while T is changed at a slow constant rate and θ_i is permanently aligned so that $85° < \Delta < 95°$. Typical T rates are between 20 and 2 mK/min; mostly cooling runs starting in the isotropic phase are conducted since the free surface often becomes macroscopically rough, thereby scattering the reflected beam, below the bulk transition to the liquid-crystal phase (this behavior is especially pronounced at isotropic to smectic-A transitions).

III. RESULTS AND DISCUSSION

A. Compounds with isotropic-nematic transition

The compounds of the $\bar{n}.O.\bar{6}$ series with $n \leqslant 10$ show isotropic to nematic transitions. Figure 3 shows the temperature dependence of the ellipticity coefficient $\bar{\rho}$ for the homologs with $n = 10,8,6,4$. All compounds show a pretransitional increase of $\bar{\rho}$ as the bulk transition to the nematic phase is approached from above. The increase of $\bar{\rho}$ is accompanied by a decrease of the Brewster angle θ_B as is exemplified in Fig. 4. At the transition, $\bar{\rho}$ shows a sharp drop and in the nematic phase range only a slight temperature variation of $\bar{\rho}$ is observed. In some cases the $\bar{\rho}$ vs T curve exhibits slight oscillations. Although these oscillations are reproducible in subsequent cooling and heating runs, they change or vanish when material is added to or removed from the sample holder or when the same compound is filled into another sample holder. These oscillations are thus not an intrinsic property of a certain compound, rather they result from the experimental conditions of a given sample–sample-holder combination; a possible origin is interference with residual light reflected at the rough sample-substrate interface.

A direct interpretation of the ellipsometric data is possible only on a qualitative and approximate level. The pretransitional increase of $\bar{\rho}$ indicates an increase of the nematic coverage Γ as the bulk transition is approached from above. It is obvious that this increase of $\bar{\rho}$ becomes less pronounced with decreasing n, suggesting a possible change from complete to partial wetting. However, for a more in-depth analysis we have to compare, as usual in ellipsometry, the experimentally measured values of the ellipsometric quantities with calculated values resulting from model structures. As is shown in the following, it turns out that the results for all compounds are in agreement with a phenomenological model predicting complete wetting with a logarithmic divergence of Γ.

There are several theoretical models [1,30–36] of the wetting behavior above isotropic-nematic transitions although most of them deal with an interface to a solid wall rather

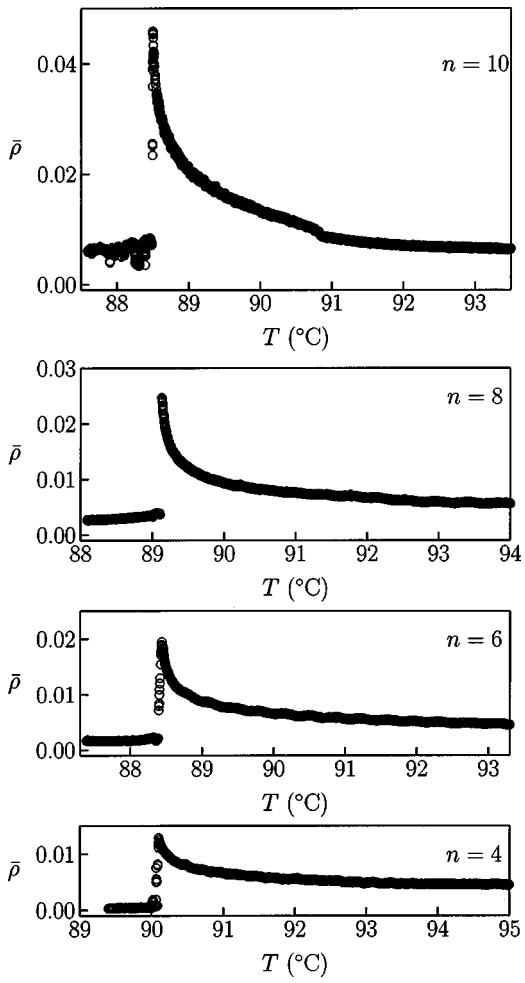

FIG. 3. Temperature dependence of the ellipticity coefficient $\bar{\rho}$ of four nematic $\bar{n}.\mathrm{O}.\bar{6}$ compounds near the bulk nematic-isotropic transition (shown is a temperature interval from about 1 K below to about 5 K above the bulk transition temperature).

than a free surface. Following the procedure described in [16], we use the model of Sheng [32] to generate temperature-dependent order parameter profiles resulting in calculated $\bar{\rho}(T)$ curves that are compared with our experimental data. Using the notation given in [16], the Landau free energy of the bulk nematic-isotropic transition, g_b, is extended by a coupling of the nematic order parameter S to a surface potential V:

$$g = g_b - V\delta(z)S + \frac{L}{2}\left(\frac{\partial S}{\partial z}\right)^2. \tag{7}$$

Here, z is the distance from the surface, and the last term with coefficient L represents the elastic energy corresponding to a z variation of S; g_b is given by the usual expansion,

$$g_b = \tfrac{1}{2}a(T-T^*)S^2 - \tfrac{1}{3}BS^3 + \tfrac{1}{4}CS^4, \tag{8}$$

where a, B, and C are positive constants and T^* gives the stability limit of the isotropic phase. The bulk transition temperature T_c and the corresponding value S_c of the bulk order parameter at T_c are given by

$$T_c = T^* + \frac{2B^2}{9aC}, \tag{9}$$

$$S_c = \frac{2B}{3C}. \tag{10}$$

Minimization of g, as described in [32,16], gives the order parameter profile $S(z)$ as a function of temperature T. If at T_c the order parameter at the surface, S_0, is larger than the bulk value S_c, the model predicts complete wetting and a logarithmic divergence of the coverage Γ at T_c. For a certain range of parameters, $S_0(T)$ and $\Gamma(T)$ show a discontinuous change at a temperature slightly above T_c corresponding to a prewetting transition. If $S_0 < S_c$ at T_c, the model predicts partial wetting and a finite Γ at T_c.

In order to calculate ellipsometric data, the $S(z)$ profile is transformed into refractive index profiles $n_e(z)$ and $n_o(z)$ as described in [16]. Invoking the roughness of the free surface by a function $d_\gamma(z)$,

$$d_\gamma(z) = \frac{1}{2}\left[1 + \tanh\left(\frac{z}{\gamma}\right)\right], \tag{11}$$

with γ being a material-dependent length (typically of the order of 1 nm), the permittivities $\epsilon_i(z) = n_i^2(z)$ are related to $S(z)$ as

$$\epsilon_e(z) = 1 + d_\gamma(z)\{[\epsilon_{iso} + \tfrac{2}{3}\Delta\epsilon_{max}S(z)] - 1\}, \tag{12}$$

$$\epsilon_o(z) = 1 + d_\gamma(z)\{[\epsilon_{iso} - \tfrac{1}{3}\Delta\epsilon_{max}S(z)] - 1\}, \tag{13}$$

where ϵ_{iso} is the permittivity of the isotropic bulk and $\Delta\epsilon_{max}$ represents the difference $(\epsilon_e - \epsilon_o)$ for $S=1$. The calculation of $\bar{\rho}$ is done via the usual multilayer approximation: a given $\epsilon(z)$ profile is divided into 500 layers and within each layer $\epsilon_o(z)$ and $\epsilon_e(z)$ are approximated by constant mean values. For the resulting multilayer system, $\Delta(\theta_i)$ and $\Psi(\theta_i)$ are calculated using the recursive formalism given by Crook [37], which can easily be extended to anisotropic layers provided the optical axis of each layer is oriented parallel to the layer normal.

Experimentally, we can determine ϵ_{iso} from the value of θ_B far above (>10 K) the nematic to isotropic bulk transition. Furthermore, the value of θ_B measured just below the bulk transition enables the determination of the permittivity

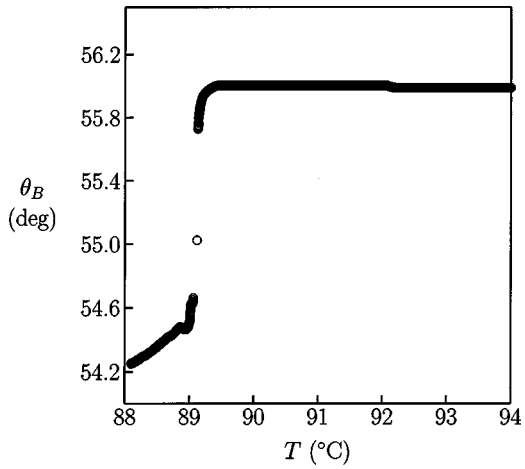

FIG. 4. Temperature dependence of the Brewster angle θ_B near the bulk nematic-isotropic transition of the compound $\bar{8}.\mathrm{O}.\bar{6}$.

TABLE II. Brewster angles at T_c+10 K ($\theta_{B,iso}$) and $T_c-0.1$ K ($\theta_{B,c}$), and permittivities at T_c+10 K (ϵ_{iso}) and $T_c-0.1$ K ($\epsilon_{e,c}, \epsilon_{o,c}$) for homologous $\overline{n}.\mathrm{O}.\overline{6}$ compounds.

Compound	$\theta_{B,iso}$ (deg)	ϵ_{iso}	$\theta_{B,c}$ (deg)	$\epsilon_{e,c}$	$\epsilon_{o,c}$
$\overline{4}.\mathrm{O}.\overline{6}$	56.08	2.211	54.90	2.326	2.152
$\overline{6}.\mathrm{O}.\overline{6}$	55.98	2.193	54.80	2.304	2.137
$\overline{8}.\mathrm{O}.\overline{6}$	55.93	2.187	54.65	2.307	2.126
$\overline{10}.\mathrm{O}.\overline{6}$	55.80	2.167	54.25	2.307	2.094
$\overline{12}.\mathrm{O}.\overline{6}$	55.91	2.184	53.94	2.372	2.091
$\overline{14}.\mathrm{O}.\overline{6}$	55.67	2.167	53.77	2.316	2.059
$\overline{16}.\mathrm{O}.\overline{6}$	55.73	2.143	53.90	2.320	2.068
$\overline{18}.\mathrm{O}.\overline{6}$	55.67	2.146	53.89	2.310	2.065
$\overline{20}.\mathrm{O}.\overline{6}$	55.62	2.137	53.89	2.289	2.059

values $\epsilon_{e,c}$ and $\epsilon_{o,c}$ at the bulk transition temperature T_c [38]; the difference $\Delta\epsilon_c=\epsilon_{e,c}-\epsilon_{o,c}$ is needed for the quantity $\Delta\epsilon_{max}$ of Eqs. (12) and (13), which can be obtained from $\Delta\epsilon_c$ using the value of the nematic bulk order parameter just below the bulk transition, S_c: $\Delta\epsilon_{max}=\Delta\epsilon_c/S_c$ with S_c given by Eq. (10). Table II gives the values of the experimentally determined optical quantities.

Assuming that the value of $\overline{\rho}$ at a temperature 10 K above the bulk transition is determined solely by the surface roughness, we can also get an experimental estimation of the surface width parameter γ from calculations using a Fermi profile as given by Eq. (5). These γ values seem to indicate an increase of the surface roughness from $\gamma=1.1$ nm to 1.6 nm with increasing chain length; however, when fitting the parameters of the Landau model to the experimental $\overline{\rho}(T)$ curves, the best results are obtained with nearly the same value $\gamma\approx 0.9$ to 1.0 nm for all compounds. Obviously, the $\overline{\rho}$ values, even at temperatures $\geqslant 10$ K above the bulk transition, still contain contributions from both $\overline{\rho_0}$ (surface roughness) and $\overline{\rho_\Gamma}$ (nematic excess surface order).

The parameters of the Landau free energy expansion (a, B, C, V, L) are varied until an order parameter profile $S(z,T)$ is obtained which results, in connection with the optical quantities given in Table II, in refractive index profiles $n_e(z,T)$ and $n_o(z,T)$ yielding a calculated $\overline{\rho}(T)$ curve reproducing the experimental $\overline{\rho}(T)$ values. The result is shown in Fig. 5, giving measured and calculated $\overline{\rho}$ values on a logarithmic temperature scale. The actual fitting process was done by minimizing the sum of the mean square deviations with starting values taken from [16]. We found that the relation between the parameter values and the quality of the fits is not ambiguous, i.e., for a given compound there are not various sets of parameters resulting in identical fits. It seems that there is a general deviation between calculated and measured $\overline{\rho}$ vs T curves which could not be removed by adjusting the parameters of the Landau model: especially in the case of $\overline{8}.\mathrm{O}.\overline{6}$ and $\overline{10}.\mathrm{O}.\overline{6}$, the curvature of the calculated curves is clearly too large in the range $T-T_c<1$ K. This observation might indicate a need of additional terms in Eq. (7) or Eq. (8) for an exact description of the experimental behavior. However, when examining the variation of the Landau parameters with the alkyl chain length n (see Fig. 6), some clear trends become obvious, especially for the parameters a, L, and V that have a simple physical meaning.

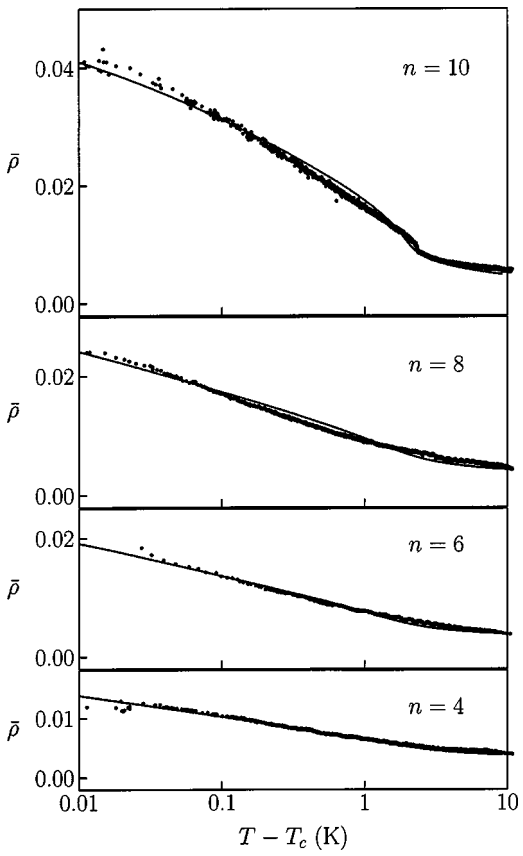

FIG. 5. Measured (small dots) and calculated (solid lines) $\overline{\rho}$ values as a function of the temperature difference from the bulk nematic-isotropic transition temperature T_c (logarithmic scale) of four nematic $\overline{n}.\mathrm{O}.\overline{6}$ compounds. The solid lines were calculated on the basis of the Landau model (see text) using the parameter values shown in Fig. 6 below.

The coefficient a, which is a measure of the inverse susceptibility of the order parameter, shows a pronounced increase with decreasing chain length. Thus, the influence of external ''fields'' inducing nematiclike order in the isotropic phase becomes weaker with decreasing chain length. This behavior is reflected by the experimental observation of the weaker pretransitional increase of $\overline{\rho}$ in shorter homologs.

The coefficient L describes the energy change resulting from an order parameter variation in the direction of the surface normal. The magnitude of L is a measure of the correlation length [32] and is related to the sum of the nematic elastic constants $k_{11}+k_{22}+k_{33}$ [16]. The observed pronounced increase of L with increasing chain length n thus indicates an increase of the elastic constants in longer homologs (which is to be expected because of the increasing tendency to form smectic phases).

Concerning the surface potential V, which is a measure of the ordering influence of the surface, the experimental results can be described with nearly the same value of V for all compounds. For a free surface, one possible origin of the excess surface order consists of the surface tension. Since the magnitude of the surface tension depends mainly on the structure and the type of atoms of the alkyl chains and less on the length of the chains [39], it is reasonable that the

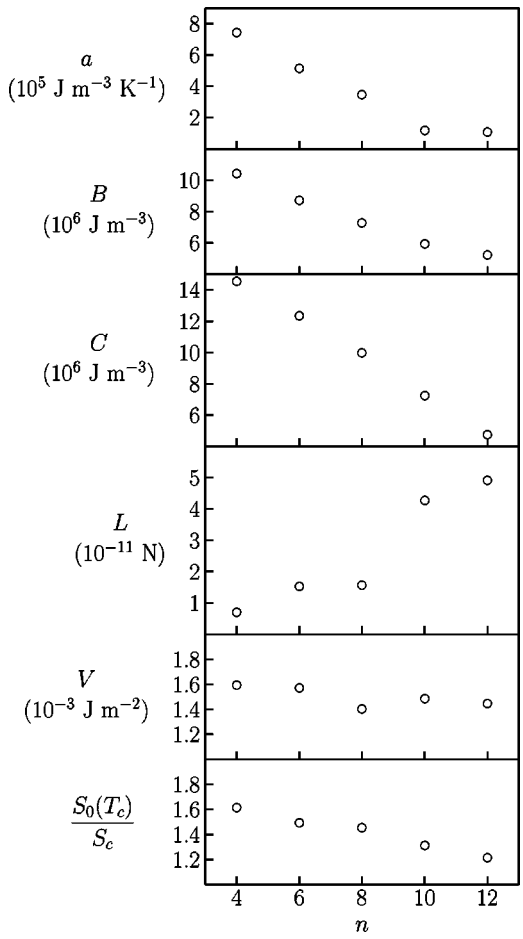

FIG. 6. Variation of the Landau parameters and the surface to bulk order parameter ratio $S_0(T_c)/S_c$ at T_c with alkyl chain length n of homologous $\overline{n}.O.\overline{6}$ compounds. Although $\overline{12}.O.\overline{6}$ shows a smectic-A–isotropic transition, its wetting behavior can be described using the parameter values given above (see Fig. 8 below).

value of V does not show a pronounced dependence on the chain length n.

Figure 6 also gives the ratio of $S_0(T_c)$, the surface order parameter at $T=T_c$, and S_c, the bulk order parameter at $T=T_c$. The value of $S_0(T_c)/S_c$ for all compounds is larger than unity and it increases with decreasing n. Thus, according to the Landau description all compounds show complete wetting and the smaller pretransitional increase of $\overline{\rho}$ in shorter homologs does not indicate a change from complete to partial wetting but just a weaker divergence (because of the smaller susceptibility a^{-1}) of the nematic coverage. We should note that our conclusion of complete wetting is mainly based on the Landau description of the experimental data. Because of the nonmonotonic relation between $\overline{\rho}$ and Γ at large Γ values a divergence of Γ is very difficult to prove by ellipsometry. What we can directly conclude from our ellipsometric data is just that they do not exclude the possibility of complete wetting.

Alkylcyanobiphenyl (nCB) liquid crystals represent the only other homologous series in which nematic wetting at the free surface has been studied. Measurements were conducted at the free surface [17,18] and at the interface to a solid substrate [5]. Whereas all studies show that the pretransitional increase of the nematic coverage becomes less pronounced in shorter homologs, the results concerning the distinction between partial and complete wetting and the dependence of $S_0(T_c)/S_c$ on the chain length n are not completely conclusive. In [17] partial wetting was observed for $n=5$ and complete wetting for $n=6,7,8$; the ratio $S_0(T_c)/S_c$ was determined for $n=7,8$, and for both compounds the same value of 1.35 was found. In [18] complete wetting was found for all compounds in the range from $n=5$ to 12 (one should note that nCB compounds with $n=10,12$ exhibit no nematic phase but an isotropic to smectic-A transition). Comparing either the even-numbered ($n=6,8,10,12$) or the odd-numbered ($n=7,9,11$) nCB compounds (in order to avoid odd-even effects), the ratio $S_0(T_c)/S_c$ shows an increase with decreasing n similar to that observed here for the $\overline{n}.O.\overline{6}$ compounds, but 5CB does not fit into this n dependence since a smaller value (1.19) was determined than for 7CB (1.30). In [5], where the interface to a silane coated glass substrate was studied, again complete wetting for $n=6$ to 9 was found but partial wetting for $n=5$, in connection with $S_0(T_c)/S_c<1$ for 5CB.

Thus, all measurements show that the pretransitional increase of the nematic coverage becomes less pronounced with decreasing chain length n, but it is not clear whether this behavior indicates a change from complete to partial wetting or just a decrease of the nematic susceptibility of the isotropic phase. The latter reason is favored by our results which are based on the Landau description of the measurements. Since we did not achieve, especially for $\overline{8}.O.\overline{6}$ and $\overline{10}.O.\overline{6}$, a perfect agreement between calculated and measured $\overline{\rho}$ values, this conclusion is not completely unambiguous. Nevertheless, for reasons given in the following section, it seems that at least the general dependence of the Landau parameters on the chain length n observed by us is consistent.

B. Compounds with isotropic–smectic-A transition

Figure 7 shows the temperature dependence of $\overline{\rho}$ for the five compounds with $n=12,14,16,18,20$ which show a direct isotropic to smectic-A transition. All smectic compounds show a pronounced pretransitional increase of $\overline{\rho}$ followed by a sharp drop at the bulk transition to the smectic-A phase. Note that the $\overline{\rho}$ value of the bulk smectic-A phase is significantly smaller than the $\overline{\rho}$ value of the bulk nematic phase (with the exception of $\overline{4}.O.\overline{6}$), indicating a smaller roughness or width (smaller $\overline{\rho_0}$ value) of the free smectic-A surface.

The compound $\overline{12}.O.\overline{6}$ obviously possesses a particular position in the $\overline{n}.O.\overline{6}$ series. This homolog is the shortest of the series that does not possess a nematic phase but a direct isotropic to smectic-A transition. The temperature dependence of $\overline{\rho}$, however, shows features that are displayed neither by the other smectic compounds ($n>12$) nor by the nematic compounds ($n\leqslant 10$). Whereas all other smectic compounds exhibit a more or less pronounced steplike growth of $\overline{\rho}$ as the bulk isotropic–smectic-A transition is approached from above, the value of $\overline{\rho}$ of $\overline{12}.O.\overline{6}$ remains nearly constant until, at a temperature 1 K above the bulk transition, a sharp jump of $\overline{\rho}$ occurs, which is followed by a

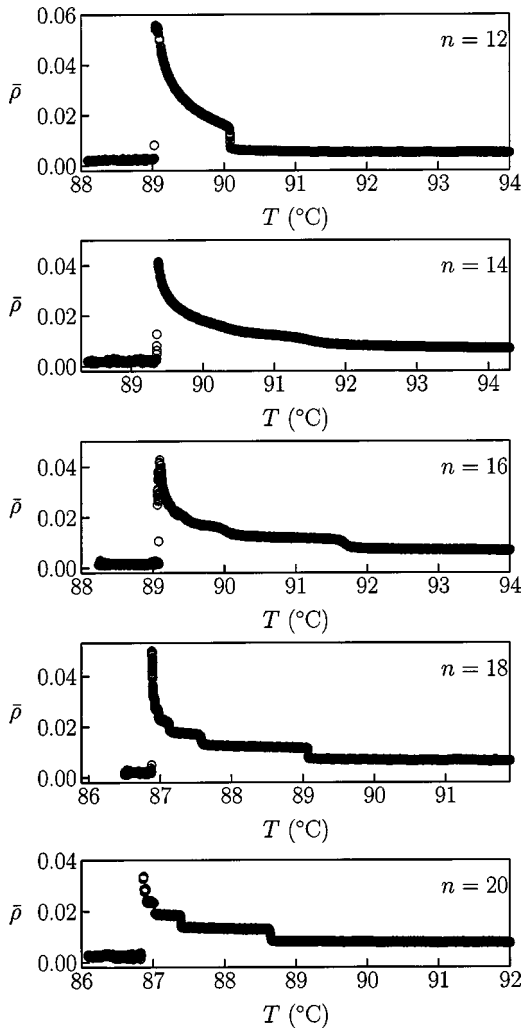

FIG. 7. Temperature dependence of the ellipticity coefficient $\bar{\rho}$ of five smectic $\overline{n}.\mathrm{O}.\overline{6}$ compounds near the bulk smectic-*A*–isotropic transition (shown is a temperature interval from about 1 K below to about 5 K above the bulk transition temperature).

pronounced continuous increase. Approximating the surface phase by a homogeneous slab with constant refractive index values as given in Table II, the jump in $\bar{\rho}$ corresponds to a surface phase thickness change of about two molecular lengths.

We have interpreted the discontinuity of $\bar{\rho}$, indicating a thickness change of the wetting layer, as a prewetting transition; details are reported in [24,26]. Here, we want to point out that the experimentally observed behavior of $\overline{12}.\mathrm{O}.\overline{6}$ is predicted by the Landau model if we extrapolate the chain length dependence of the Landau parameters obtained for the nematic compounds ($n=4$ to 10) to $n=12$: Fig. 8 shows the calculated $\bar{\rho}$ vs T curve, resulting from a least-mean-square fit, together with the measured $\bar{\rho}$ values of $\overline{12}.\mathrm{O}.\overline{6}$ (the different curvatures at $T-T_c<1$ K, which we already noted for $\overline{8}.\mathrm{O}.\overline{6}$ and $\overline{10}.\mathrm{O}.\overline{6}$, are now most obvious). The corresponding Landau parameters are well in agreement with the *n* dependencies of the nematic compounds (see Fig. 6). Since $\overline{12}.\mathrm{O}.\overline{6}$ shows an isotropic to smectic-*A* transition, the Landau model is in a strict sense not applicable to $\overline{12}.\mathrm{O}.\overline{6}$. On the other hand, one might argue that the smectic ordering in

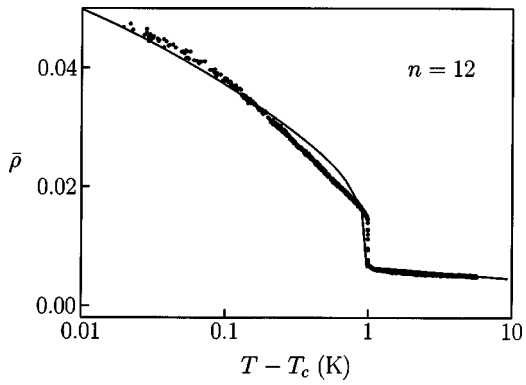

FIG. 8. Measured (small dots) and calculated (solid line) $\bar{\rho}$ values as a function of the temperature difference from the bulk smectic-*A*–isotropic transition temperature T_c (logarithmic scale) of the compound $\overline{12}.\mathrm{O}.\overline{6}$. The solid line was calculated on the basis of the Landau model (see text) using the parameter values shown in Fig. 6.

$\overline{12}.\mathrm{O}.\overline{6}$ is just a small modulation. This is indicated by the absence of the pretransitional layer-by-layer growth observed for the longer homologs and by the observation that a nematic phase appears when $\overline{12}.\mathrm{O}.\overline{6}$ is doped with a small amount (≈ 2.5 mol %) of a second smectic compound [26], i.e., the smectic order vanishes due to a small distortion. Thus, if the main part of the order parameter of the isotropic–smectic-*A* transition is still represented by the nematic orientational order, the Landau model might still be used, to some extent, for the description of the wetting behavior of $\overline{12}.\mathrm{O}.\overline{6}$.

However, the chain length dependence of the Landau parameters shown in Fig. 6 gives a consistent description of the experimental wetting behavior of the compounds with $n=4$ to 12. According to the Landau model, the appearance of the prewetting transition in $\overline{12}.\mathrm{O}.\overline{6}$ is mainly due to the increase of the coefficient *L*, which is a measure of the energy connected with the spatial variation of the order parameter *S*. Since the value of the Landau parameter *V*, representing the surface potential acting on the molecules, changes only slightly with increasing chain length *n*, whereas the critical value V_c, below which a prewetting transition occurs, varies as $V_c \propto \sqrt{L}$ [33] and thus increases with increasing chain length *n*, *V* is for $\overline{12}.\mathrm{O}.\overline{6}$ obviously smaller than V_c (the small kink, which is observed in the $\bar{\rho}$ vs *T* curve of $\overline{10}.\mathrm{O}.\overline{6}$, may indicate that for this compound already $V \approx V_c$).

For the other smectic compounds ($n \geq 14$) the positional smectic order is an essential part of the order parameter of the isotropic to smectic-*A* transition and the ''nematic'' Landau model is not applicable. Extrapolating the *n* dependence of the Landau parameters to larger ($n>12$) values would result in a larger prewetting discontinuity, a shift of the prewetting transition temperature toward the bulk transition, and finally to partial wetting, lacking almost completely a pretransitional increase of the surface coverage. Instead, we observe that a prewetting transition is not present in the compounds with $n \geq 14$ and that all compounds show a pronounced pretransitional increase of $\bar{\rho}$. The most striking feature of the smectic compounds is the appearance of layering steps in the growth of the wetting film, a behavior which is

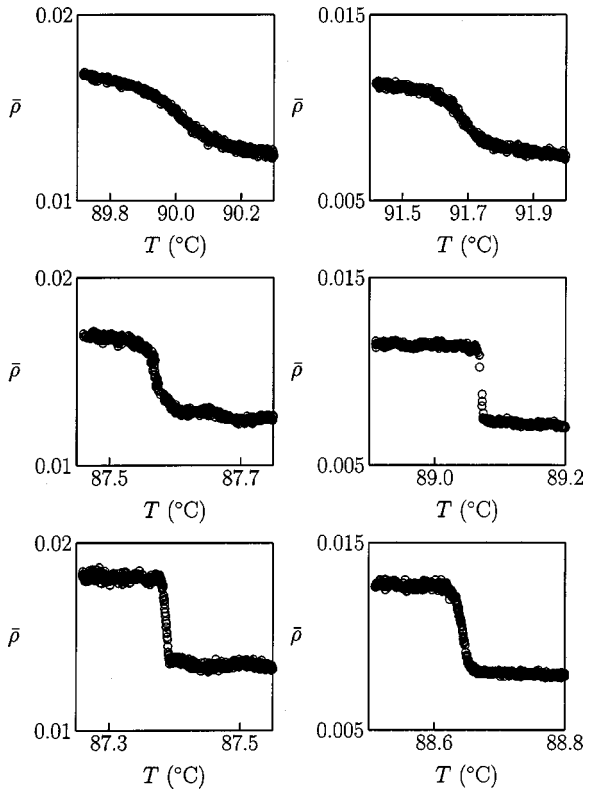

FIG. 9. Comparison of different layering steps of three homologous $\overline{n}.\mathrm{O}.\overline{6}$ compounds; upper line, $n=16$; middle line, $n=18$; lower line, $n=20$; left column, $2\leftrightarrow3$ step; right column, $1\leftrightarrow2$ step.

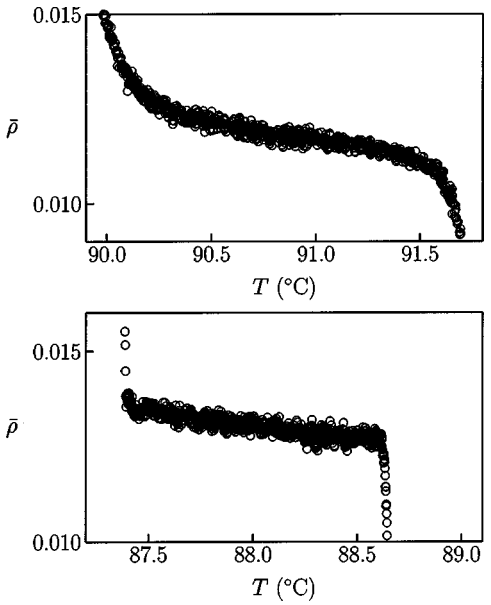

FIG. 10. Temperature dependence of the ellipticity coefficient $\overline{\rho}$ between the $1\leftrightarrow2$ and $2\leftrightarrow3$ layering steps of the compounds $\overline{16}.\mathrm{O}.\overline{6}$ (upper diagram) and $\overline{20}.\mathrm{O}.\overline{6}$ (lower diagram).

well known from smectic *n*CB and *n*OCB compounds [21–23].

It seems to be a general tendency that the layering steps, which are almost not discernible in $\overline{14}.\mathrm{O}.\overline{6}$, become sharper with increasing *n*. When comparing certain steps in different compounds [40], however, a more differentiated behavior is seen: Fig. 9 shows the one layer to two layer ($1\leftrightarrow2$) and two layer to three layer ($2\leftrightarrow3$) steps for $\overline{16}.\mathrm{O}.\overline{6}$, $\overline{18}.\mathrm{O}.\overline{6}$, and $\overline{20}.\mathrm{O}.\overline{6}$. The $1\leftrightarrow2$ step is clearly continuous in $\overline{16}.\mathrm{O}.\overline{6}$, then shows a discontinuous appearance in $\overline{18}.\mathrm{O}.\overline{6}$, but in $\overline{20}.\mathrm{O}.\overline{6}$ it seems to be again continuous (but steeper than in $\overline{16}.\mathrm{O}.\overline{6}$). In contrast, the $2\leftrightarrow3$ step (and all ''higher'' steps) shows a monotonic tendency to become sharper with increasing *n*. Theories of surface-induced ordering above smectic-*A*–isotropic transitions predict that layering steps are disfavored close to and far away from the isotropic–nematic–smectic-*A* (*I-N-A*) triple point [35,41,42]. Near the *I-N-A* point, i.e., at shorter chain length *n*, this behavior has already been experimentally confirmed for *n*CB and *n*OCB compounds [21,22], but the behavior far away from the *I-N-A* point, i.e., at very long alkyl chain lengths, has scarcely been studied experimentally. The slight ''softening'' observed here for the $1\leftrightarrow2$ step in $\overline{20}.\mathrm{O}.\overline{6}$ compared to $\overline{18}.\mathrm{O}.\overline{6}$ might indicate the theoretically predicted behavior far away from the *I-N-A* point. Also, the differences between the $1\leftrightarrow2$ and $2\leftrightarrow3$ steps (the $2\leftrightarrow3$ ''softens'' apparently at larger *n* than the $1\leftrightarrow2$ step) are in agreement with theoretical predictions [42], but for a definite conclusion studies of still longer homologs or of compounds with a larger smectic order parameter are needed.

The sharpening of the layering steps indicates that with increasing *n* the growth of the wetting film becomes more and more dominated by the positional order of the molecules, i.e., the wetting film does not grow by continuously expanding the nematic orientational order from the surface to the bulk phase, rather it grows by adding single smectic layers to the surface phase. There is, however, even in $\overline{20}.\mathrm{O}.\overline{6}$ a residual growth of $\overline{\rho}$ in the ''plateau'' between two layering steps, as can be seen in Fig. 10 showing the temperature dependence of $\overline{\rho}$ between the $1\leftrightarrow2$ and $2\leftrightarrow3$ layering steps. In this region of small wetting film thickness, the relation between $\overline{\rho}$ and the coverage Γ is still linear. An increase of $\overline{\rho}$ is thus a direct measure of an increase of Γ [Eq. (6)] or, in the approximation of a homogeneous slab model, of the product $h\Delta\epsilon$ (h being the thickness of the wetting film and $\Delta\epsilon$ the difference ϵ_e-ϵ_o). The probable origin of the increase of $\overline{\rho}$ between the layering steps is an increase of both the positional and orientational molecular order within the smectic layers, resulting in an increase of $\Delta\epsilon$ and maybe a slight increase of the layer thickness.

Comparing the temperature dependence of $\overline{\rho}$ of the different smectic compounds (Fig. 7), it is obvious that the temperatures of the layering steps shift toward the bulk transition temperature with increasing *n*. Figure 11 shows the temperature difference from the bulk transition of all steps (except the $0\leftrightarrow1$ steps; see [40]) that are discernible in the compounds $\overline{16}.\mathrm{O}.\overline{6}$, $\overline{18}.\mathrm{O}.\overline{6}$, and $\overline{20}.\mathrm{O}.\overline{6}$. The presence of the layering steps in the smectic compounds gives us also a direct measure of the thickness of the wetting film: If we make the approximation that in a given compound all layers have the same thickness and that other contributions to the coverage Γ than an integral number of smectic layers may be neglected, we can read the wetting film thickness directly from the ellipsometric data. The data shown in Fig. 11 thus also represent the temperature dependence of Γ or wetting film thickness. Nevertheless, the distinction between com-

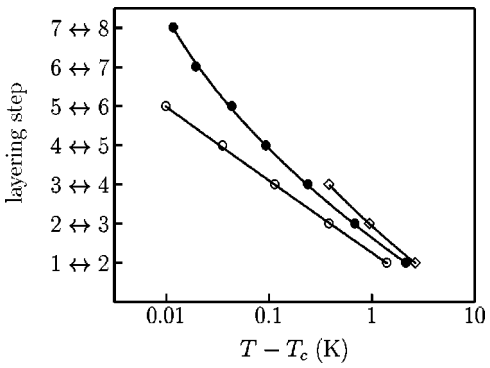

FIG. 11. Discernible layering steps of the compounds $\overline{16}.O.\overline{6}$ ($\diamond$ symbols), $\overline{18}.O.\overline{6}$ ($\bullet$ symbols), and $\overline{20}.O.\overline{6}$ ($\circ$ symbols) as a function of the temperature difference from the bulk smectic-*A*–isotropic transition temperature T_c (logarithmic scale); solid lines are just guides to the eye.

plete and partial wetting for the smectic compounds suffers from the same problem as in the nematic case, namely, the nonmonotonic relation between $\overline{\rho}$ and Γ. Even if the layering steps were not smeared out, they would not be discernible around the maximum of the $\overline{\rho}(\Gamma)$ function and a divergence of Γ would be difficult to prove. Thus, our ellipsometric data do not exclude complete wetting for the smectic compounds, but there seems to be an indication of a possible partial wetting behavior of the longest homolog, $\overline{20}.O.\overline{6}$.

Comparing the number of observable steps in $\overline{18}.O.\overline{6}$ and $\overline{20}.O.\overline{6}$, it is obvious that the number of steps decreases from $n=18$ to $n=20$. This could be due to the limited experimental temperature resolution, i.e., the longer the chain length *n*, the larger the number of steps that are quenched into a narrow (<5 mK) temperature interval above the bulk transition. A different origin might be that the number of steps really decreases with increasing *n* because the wetting behavior either changes from complete to partial or, if the wetting is partial anyway, adopts an increasingly ''nonwettinglike'' character. The data obtained for $\overline{18}.O.\overline{6}$ do not exclude complete wetting (as is discussed in detail in [27]), but the subtle change of the curvature of the solid lines in Fig. 11 might indicate a change to partial wetting with increasing chain length *n*. Thus, it may be that $\overline{20}.O.\overline{6}$ shows just six layering steps and the wetting film consists at the bulk transition temperature of six smectic layers. Clearly, partial wetting (only two smectic layers at the bulk transition) was also observed for long *n*OBC homologs [22].

IV. CONCLUSION

We have presented a detailed ellipsometric study of the wetting behavior at the free surface of nine homologous liquid-crystal compounds ($\overline{n}.O.\overline{6}$, with alkyl chain length *n* in the range from 4 to 20) above their isotropic to nematic or isotropic to smectic-*A* transition. All compounds show a surface-induced liquid-crystal phase in the temperature range of the isotropic bulk phase. The thickness of this liquid-crystal wetting film increases as the bulk transition temperature is approached from above. Concerning the variation of the wetting behavior with alkyl chain length, our results resemble most observations made in earlier studies of the free surface of homologous *n*CB, *n*OCB, and PCH*n* compounds [15–18,21–23].

For the four compounds showing an isotropic-nematic transition ($n=4$ to 10), the pretransitional increase of the nematic coverage clearly becomes less pronounced with decreasing *n*, indicating on first sight a possible change from complete to partial wetting. However, the results of all nematic compounds can be consistently described by a Landau model yielding complete wetting; the ratio $S_0(T_c)/S_c$, which determines the wetting behavior of the model (complete wetting is obtained for $S_0(T_c)/S_c>1$), increases linearly with decreasing *n* from 1.31 at $n=10$ to 1.61 at $n=4$. The observed weakness of the pretransitional increase of the wetting film thickness in short homologs is explained by the model by a decrease of the nematic susceptibility a^{-1} with decreasing *n*.

The decrease of $S_0(T_c)/S_c$ with increasing *n*, indicating a change from complete to partial wetting at longer chain lengths, is mainly due to the increase of the elastic coefficient *L*, describing the energy associated with a spatially varying nematic order parameter $S(z)$. Near the change from complete to partial wetting, the model predicts the occurrence of a prewetting transition, which is indeed observed experimentally in the ''first'' compound ($n=12$) possessing a direct isotropic to smectic-*A* transition. The experimental results for this compound can still be described by the nematic Landau model, indicating that the nematic orientational order represents the major part of the order parameter of the isotropic–smectic-*A* transition in $\overline{12}.O.\overline{6}$ (although the increase of *L* is probably due to the appearance of smectic positional order).

The wetting behavior of the longer smectic homologs ($n=14$ to 20) is influenced by the smectic positional order, as is seen from the appearance of layering steps in the pretransitional increase of the wetting film thickness. The steps are considerably smeared out in $\overline{14}.O.\overline{6}$ and $\overline{16}.O.\overline{6}$, but clearly discernible in $\overline{18}.O.\overline{6}$ and $\overline{20}.O.\overline{6}$, thereby confirming theoretical predictions that layering transitions are disfavored near *I-N-A* triple points. The observation that the $1\leftrightarrow 2$ step appears less steep again in $\overline{20}.O.\overline{6}$ than in $\overline{18}.O.\overline{6}$ might be seen as an indication that the same behavior occurs, as theoretically predicted, far away from *I-N-A* points. The step temperatures shift toward the bulk transition temperatures with increasing *n*, thereby reducing the number of observable steps from eight in $\overline{18}.O.\overline{6}$ to six in $\overline{20}.O.\overline{6}$. A comparison of the step temperatures of $\overline{18}.O.\overline{6}$ and $\overline{20}.O.\overline{6}$ on a logarithmic temperature scale indicates that very long smectic homologs probably show partial wetting, whereas ellipsometry does not allow a definite distinction between complete and partial wetting for the shorter smectic homologs.

Future studies could address the structure of the liquid-crystal wetting film of the compounds near the *I-N-A* point where the smectic compounds do not show layering steps and the prewetting transition occurs. We have started x-ray reflectivity studies of the corresponding $\overline{n}.O.\overline{6}$ compounds.

ACKNOWLEDGMENTS

This work was supported by the Deutsche Forschungsgemeinschaft (Grant No. Ba1048/5) and the Fonds der Chemischen Industrie.

[1] T. J. Sluckin and A. Poniewierski, in *Fluid Interfacial Phenomena*, edited by C. A. Croxton (Wiley, Chichester, 1986), p. 215, and references therein.
[2] B. Jérôme, Rep. Prog. Phys. **54**, 391 (1991), and references therein.
[3] K. Miyano, Phys. Rev. Lett. **43**, 51 (1979).
[4] H. Hsiung, Th. Rasing, and Y. R. Shen, Phys. Rev. Lett. **57**, 3065 (1986).
[5] W. Chen, L. J. Martinez-Miranda, H. Hsiung, and Y. R. Shen, Phys. Rev. Lett. **62**, 1860 (1989).
[6] P. Pieranski and B. Jérôme, Phys. Rev. A **40**, 317 (1989).
[7] B. M. Ocko, Phys. Rev. Lett. **64**, 2160 (1990).
[8] G. P. Crawford, R. J. Ondris-Crawford, S. Žumer, and J. W. Doane, Phys. Rev. Lett. **70**, 1838 (1993).
[9] G. P. Crawford, R. J. Ondris-Crawford, J. W. Doane, and S. Žumer, Phys. Rev. E **53**, 3647 (1996).
[10] M. P. Valignat, S. Villette, J. Li, R. Barberi, R. Bartolino, E. Dubois-Violette, and A. M. Cazabat, Phys. Rev. Lett. **77**, 1994 (1996).
[11] S. Bardon, R. Ober, M. P. Valignat, F. Vandenbrouck, A. M. Cazabat, and J. Daillant Phys. Rev. E **59**, 6808 (1999).
[12] B. Alkhairalla, H. Allinson, N. Boden, S. D. Evans, and J. R. Henderson, Phys. Rev. E **59**, 3033 (1999).
[13] M. G. J. Gannon and T. E. Faber, Philos. Mag. A **37**, 117 (1978).
[14] The abbreviation *n*CB refers to homologous 4-alkyl-4′-cyanobiphenyl compounds with *n* giving the number of carbon atoms in the alkyl chain.
[15] D. Beaglehole, Mol. Cryst. Liq. Cryst. **89**, 319 (1982).
[16] S. Immerschitt, T. Koch, W. Stille, and G. Strobl, J. Chem. Phys. **96**, 6249 (1992).
[17] H. Kasten and G. Strobl, J. Chem. Phys. **103**, 6768 (1995).
[18] P. de Schrijver, C. Glorieux, W. van Dael, and J. Thoen, Liq. Cryst. **23**, 709 (1997).
[19] The abbreviation PCH*n* refers to homologous 4-cyanophenyl-4′-alkylcyclohexyl compounds with *n* giving the number of carbon atoms in the alkyl chain.
[20] The abbreviation *n*OCB refers to homologous 4-alkyloxy-4′-cyanobiphenyl compounds with *n* giving the number of carbon atoms in the alkyloxy chain.
[21] B. M. Ocko, A. Braslau, P. S. Pershan, J. Als-Nielsen, and M. Deutsch, Phys. Rev. Lett. **57**, 94 (1986).
[22] P. S. Pershan, J. Phys. (Paris), Colloq. **50**, C7-1 (1989).
[23] G. J. Kellogg, P. S. Pershan, E. H. Kawamoto, W. F. Foster, M. Deutsch, and B. M. Ocko, Phys. Rev. E **51**, 4709 (1995).
[24] R. Lucht and Ch. Bahr, Phys. Rev. Lett. **78**, 3487 (1997).
[25] R. Lucht, Ch. Bahr, G. Heppke, and J. W. Goodby, J. Chem. Phys. **108**, 3716 (1998).
[26] R. Lucht and Ch. Bahr, Phys. Rev. Lett. **80**, 3783 (1998).
[27] R. Lucht, Ch. Bahr, and G. Heppke, J. Phys. Chem. B **102**, 6861 (1998).
[28] The abbreviation $\bar{n}.\mathrm{O}.\bar{6}$ refers to homologous 4-hexyloxyphenyl esters of 4-alkyloxybenzoic acid compounds with *n* giving the number of carbon atoms in the alkyloxy chain.
[29] S. N. Jasperson and S. E. Schnatterly, Rev. Sci. Instrum. **40**, 761 (1969).
[30] P. Sheng, Phys. Rev. Lett. **37**, 1059 (1976).
[31] D. W. Allender, G. L. Henderson, and D. L. Johnson, Phys. Rev. A **24**, 1086 (1981).
[32] P. Sheng, Phys. Rev. A **26**, 1610 (1982).
[33] A. Mauger, G. Zribi, D. L. Mills, and J. Toner, Phys. Rev. Lett. **53**, 2485 (1984).
[34] M. M. Telo da Gama, Mol. Phys. **52**, 611 (1984).
[35] J. V. Selinger and D. R. Nelson, Phys. Rev. A **37**, 1736 (1988).
[36] B. Tjipto-Margo, A. K. Sen, L. Mederos, and D. E. Sullivan, Mol. Phys. **67**, 601 (1989).
[37] A. W. Crook, J. Opt. Soc. Am. **38**, 954 (1948).
[38] The determination of ϵ_e and ϵ_o from the Brewster angle of the bulk liquid-crystal phase is based on the assumption that ϵ_e and ϵ_o are related to the value ϵ_{iso}, measured in the isotropic phase, as $\frac{2}{3}\epsilon_o+\frac{1}{3}\epsilon_e=\epsilon_{iso}$, i.e., the density jump at the isotropic to liquid-crystal transition and any temperature dependence of the density are neglected.
[39] P. Mach, C. C. Huang, T. Stoebe, E. D. Wedell, H. T. Nguyen, W. H. de Jeu, F. Guittard, J. Naciri, R. Shashidhar, N. A. Clark, I. M. Jiang, F. J. Kao, H. Liu, and H. Nohira, Langmuir **14**, 4330 (1998).
[40] The following discussion does not concern the first layering step at which the first smectic layer is formed at the isotropic surface. This ''step'' occurs in all compounds ($n=14$ to 20) about 15 K above the bulk transition temperature and is smeared out over a temperature interval of several kelvin.
[41] Z. Pawlowska, T. J. Sluckin, and G. F. Kventsel, Phys. Rev. A **38**, 5342 (1988).
[42] A. M. Somoza, L. Mederos, and D. E. Sullivan, Phys. Rev. E **52**, 5017 (1995).